Indian Journal of Pure & Applied Physics
Vol. 64, April 2026, pp. 425-434
DOI: 10.56042/ijpap.v64i4.27192

A Compact First-Order Mixed-Mode Multifunction Filter Architecture Using CFDITA

Anupam, Atul Kumar* & Sajai Vir Singh

Department of Electronics and Communication Engineering, Jaypee Institute of Information Technology, Noida 201 304, India

Received: 2nd January 2026; accepted: 28th January 2026

A first-order mixed-mode multifunction filter utilizing a Current Follower Differential Input Transconductance Amplifier (CFDITA) and a grounded capacitor is introduced in this paper. It can be configured to provide first-order high-pass (HP), low-pass (LP) and all-pass (AP) responses in current-mode as well as a HP response in transadmittance-mode. The filter offers advantages such as suitable impedances in both current-mode and transadmittance-mode, facilitating simple cascadability in either mode, ease of integration, minimal use of active and passive components, explicit current outputs to drive current-mode devices and the employment of a grounded capacitor that assists in parasitic absorption of the active element used. Additionally, it has a higher operating frequency (10.3 MHz), low power consumption (1.5 mW), electronic tunability of pole frequency and no need for matching passive components. A thorough analysis considering ideal, non-ideal, and parasitic effects is provided. The study also examines the use of the suggested filter as a quadrature oscillator. Post-layout simulations utilizing the Cadence Virtuoso tool with a 180 nm GPDK (Generic Process Design Kit) technology have confirmed the developed circuits. The layout of CFDITA measures an area of 28.4 µm × 26.5 µm.

Keywords: Analog circuits, Analog filter, Oscillator, Mixed-mode

1 Introduction

Current trends in analog signal processing focus on enhancing performance, energy efficiency and miniaturization through advancements in circuit design, materials and the incorporation of artificial intelligence and these developments have been complemented over recent decades by progress in current-mode (CM) active building blocks that significantly advance the implementation of active filters and oscillators. These blocks can function at greater frequencies, consume less power and exhibit superior linearity compared to voltage-mode (VM) active blocks[1-2]. This approach is particularly relevant for complex circuits and various applications where speed and efficient power usage are crucial. Due to the simpler and compact designs, low cost and power saving features, first-order filters are very popular. The low-pass (LP), high-pass (HP) and all-pass (AP) filtering responses can be accomplished in first-order filters[3-5]. LP, HP, and AP filters are essential tools in analog signal processing. LP filters smooth signals by allowing low frequencies to pass while reducing high-frequency noise, whereas HP filters remove unwanted low-frequency components such as DC offsets and slow drifts. AP filters preserve signal amplitude while adjusting phase, enabling precise phase correction without altering magnitude. These filters can be implemented in four operating modes: VM, CM, transadmittance-mode (TAM), and transimpedance-mode (TIM). VM filters process voltage signals at both input and output, CM filters operate with current signals, TAM filters convert input voltages into output currents, and TIM filters convert input currents into output voltages. The choice of active building blocks used to realize a filter is critical, as it directly determines the filter's overall performance and significantly affects key parameters such as bandwidth, linearity, and noise behavior.

The literature has documented a number of first-order filters employing different modes of operation, including CM[3-13], VM[13-25], TAM[26, 27], and mixed-mode (MM)[28-32], implemented with a wide range of active building blocks. The CM filters employ the active elements such as Dual X Current Conveyor Transconductance Amplifier (DX-CCTA)[3, 8, 11], Current Controlled Second-generation Current Conveyor (CCCII)[4], Multiple Output Current Differencing Transconductance Amplifier (MO-CDTA)[5], Extra-X Current Conveyor (EXCCII)[6, 10], Extra-X Current

*Corresponding author: E-mail: atul.nit304@gmail.com

Controlled Current Conveyor (EXCCCII)[7], CCII[9], Differential Difference Dual-X Second-generation Current Conveyor (DD-DXCCII)[12] and Multi-Output CCII (MO-CCII)[13].

The VM filters are based on active elements such as Differential Difference Current Conveyor (DDCC)[13], Voltage Differencing Inverting Buffered Amplifier (VDIBA)[14], MOS Transistors[15], Voltage Differencing Current Conveyor (VDCC)[16], Second-generation Voltage Conveyor (VCII)[17], Dual-X Second-generation Multi-Output Current Conveyor (DX-MOCCII)[18], Dual-X Second-generation Current Conveyor (DXCCII)[19], EXCCII[20], Fully Differential Second-generation Current Conveyors (FDCCII)[21], Dynamic Threshold Voltage MOSFET (DTMOS)[22], Current Feedback Operational Amplifier (CFOA)[23, 24], and DD-DXCCII[25].

In TAM, the first-order filters are designed with Voltage Differencing Voltage Transconductance Amplifier (VDVTA) and Operational Transconductance Amplifiers (OTAs)[26, 27].

In MM, filters are based on Multiple-Output DXCCTA (MO-DXCCTA)[28], Extra X Current Conveyor Transconductance Amplifier (EXCCTA)[29], VCII[30], Voltage Differencing Gain Amplifier (VDGA)[31] and Dual-X Current Conveyor Differential Input Transconductance Amplifier (DXCCDITA)[32].

The limitations observed from the study of the above-mentioned filters are given as follows

i. Requirement of different kinds of active blocks, which increase complexity and area[26, 27].
ii. Use of floating passive components and/or more passive components[6, 8-11, 14-19, 22, 31].
iii. Absence of all basic filtering responses in a single structure[8-11, 14-27, 30, 32].
iv. Lack of electronic tunability[9, 12, 13, 15, 17-20, 22-24, 30].
v. Only single-mode operation, which limits the flexibility[3-27].
vi. Inappropriate input/output impedances, which affects the cascadability[9, 16, 19].

In this context, this study seeks to add to the existing research on multifunction filter development by introducing a first-order mixed-mode multifunction filter (FO-MMMF). The suggested design realizes a compact and effective circuit implementation through the use of a Current Follower Differential Input Transconductance Amplifier (CFDITA) along with single grounded capacitor. The suggested filter is easily cascadable and works well in two different modes. It provides direct current outputs, which makes it suitable for driving other CM circuits. The use of grounded capacitor helps absorb parasitic of the active block. The circuit offers electronic tuning of pole frequency and does not require any matching constraint; has good operating frequency and consumes low power. Theoretical study and simulation findings demonstrate the effectiveness of the suggested architecture, suggesting its utility for real-world signal processing applications. Table 1 presents an overview and comparison of first-order filter performance metrics.

2 Materials and Methods

2.1 Suggested Mixed-mode Multifunction Filter

CFDITA is a basic analog block widely used in signal processing, particularly in CM circuits[33-37]. It combines the characteristics of a differential input transconductance amplifier and a current follower. Due to its broader bandwidth, better linearity and low power operability, CFDITA is helpful in the design of diverse applications like analog filters, oscillators, rectifiers, instrumentation amplifiers, multi-vibrators, etc. In the proposed filter architecture, a Z_C CFDITA is utilized. The symbol of CFDITA used in the proposed filter architecture is depicted in Fig. 1 (a), and its CMOS implemented circuit[34] is depicted in Fig.1 (b). The port relationships of CFDITA are described in the following matrix.

$$\begin{bmatrix} I_V \\ I_Z \\ I_{ZC} \\ I_{O+} \\ I_{O-} \end{bmatrix} = \begin{bmatrix} 0 & 0 & 0 \\ 0 & 0 & 1 \\ 0 & 0 & 1 \\ -g_m & g_m & 0 \\ g_m & -g_m & 0 \end{bmatrix} \begin{bmatrix} V_V \\ V_Z \\ I_F \end{bmatrix} \quad \ldots (1)$$

where $g_m = \sqrt{k_n I_B}$, ($k_n = \mu_n C_{OX} W/L$ is the physical parameter of NMOS transistor) is the transconductance of CFDITA, I_F, I_Z, I_{ZC}, I_{O+} and I_{O-} are the currents at terminal *F, Z, Z_C, O+* and *O-* respectively; V_F, V_Z, V_{ZC}, V_{O+} and V_{O-} are the voltages at terminal *F, Z, Z_C, O+* and *O-* respectively.

The implemented FO-MMMF circuit is shown in Fig. 2. It may be configured to produce an HP response in TAM and HP, LP, and AP responses in CM. The suggested multifunction filter architecture employs minimum active and passive components as it uses a sole CFDITA along with a single grounded capacitor only. The incorporation of a grounded capacitor aids in the absorption of parasitic elements

Table 1 — The comparison of first-order filters' performance metrics

Ref.	ABB/Count	No. of Passive elements	All Grounded Passive elements	Availability of LP, HP and AP	Appropriate input and output impedances	Mode of operation	Configur-ation	Electronic Tuning	Technology Used (μm)	Power Supply (V)	Power Consumption (mW)	Post Layout simulations
[3]	DXCCTA/1	2C	YES	YES	YES	CM	SIMO	YES	---	±1.25	1.75	NO
[4]	CCCII/2	2C	YES	YES	YES	CM	SIMO	YES	---	±2.5	2.72	NO
[5]	MO-CDTA/1	1C	YES	YES	YES	CM	MIMO	YES	0.13	±1	2.5	NO
[6]	EXCCII/1	1R,1C	NO	YES	YES	CM	SIMO	YES	0.25	±1.25	---	NO
[7]	EXCCCII/1	1C	YES	YES	YES	CM	SIMO	YES	0.18	± 1.25	0.44 - 4.4	NO
[8]	DXCCTA/1	1C	NO	NO	YES	CM	MISO	YES	0.18	± 1.25	---	NO
[9]	CCII/2	1R,1C	NO	NO	NO	CM	SISO	NO	0.18	± 0.2	0.00053	NO
[10]	EXCCII/1	1R,1C	NO	NO	YES	CM	SISO	YES	0.18	±0.75	0.568	NO
[11]	DXCCTA/1	1C	NO	NO	YES	CM	SISO	YES	0.18	± 1.25	---	NO
[12]	DD-DXCCII/1	1C	YES	YES	YES	CM	MIMO	NO	---	± 1.25	2.5	NO
[13]	MO-CCII//2,	1R,1C	YES	YES	YES	CM	MISO	NO	0.18	± 1.25	3.71	NO
	DDCC-/2	1R,1C	YES	YES	YES	VM	MISO	NO	0.18	± 1.25	3.71	NO
[14]	VDIBA/1	1C	NO	NO	YES	VM	SIMO	YES	IC	±5	---	NO
[15]	MOS Transistor/4	1R,1C	NO	NO	YES	VM	SISO	NO	0.18	±0.9	0.54	NO
[16]	VDCC/1	2R,1C	NO	NO	NO	VM	SISO	YES	0.18	±0.9	0.492	NO
[17]	VCII/1	2R,1C	NO	NO	YES	VM	SISO	NO	0.18	± .9	0.069	NO
[18]	DX-MOCCII/1	2R,1C	NO	NO	YES	VM	SISO	NO	0.25	± 1.25	---	NO
[19]	DXCCII/1	1R,1C	NO	NO	NO	VM	SISO	NO	0.25	± 1.25	---	NO
[20]	EXCCII/1	2R,2C	YES	NO	YES	VM	SISO	NO	0.25	±1.2	0.7	NO
[21]	FDCCII/1	1C	YES	NO	YES	VM	SISO	YES	0.18	± 1.25	2	NO
[22]	DTMOS/1	1R,1C	NO	NO	YES	VM	SISO	NO	0.18	0.2	---	NO
[23]	CFOA/2	3R,1C	YES	NO	YES	VM	SISO	NO	0.18	±8	---	NO
[24]	CFOA/2	3R,1C	YES	NO	YES	VM	SISO	NO	IC	±10	---	NO
[25]	DD-DXCCII/1	1C	YES	NO	YES	VM	SIMO	YES	0.18	±1.25	---	NO
[26]	VDVTA/1, OTA/2	1C	YES	NO	YES	TAM	SISO	YES	0.18	±0.85	1.6 - 4.76	NO
[27]	VDVTA/1, OTA/1	1C	YES	NO	YES	TAM	SISO	YES	0.18	±0.85	---	NO
[28]	MO-DXCCTA/1	1C	YES	YES	YES	CM/TAM	SIMO	YES	---	± 1.25	1.4	NO
[29]	EXCCTA/1	1R,1C	YES	YES	YES	CM/VM/ TAM/ TIM	SIMO	YES	0.18	± 1.25	---	YES
[30]	VCII/2	3R,1C	YES	NO	YES	CM/TIM	SISO	NO	0.18	±0.9	1.22	NO
[31]	VDGA/1	1R,1C	NO	YES	YES	CM/VM/ TAM/ TIM	SIMO	YES	0.18	±0.9	1.31	NO
[32]	DXCCDITA/1	1C	YES	NO	YES	CM/VM/ TAM	SISO	YES	0.35	±1.5	---	NO
Proposed	CFDITA/1	1C	YES	YES	YES	CM/TAM	MIMO	YES	0.18	± 1.25	1.5	YES

within the device. The input current signal, I_{in} is applied at terminal F, which operates as a low impedance terminal; this allows the proposed filter to be cascaded in CM and TAM, with output signal currents, I_1 and I_2 explicitly accessible at high impedance terminals for easy driving of CM blocks. The input voltage signal, V_{in} is applied at the high impedance terminal V, facilitating the cascading of the proposed filter in VM and TIM. Therefore, the recommended filter's input and output impedances are appropriate for both CM and TAM applications. The standard circuit analysis is conducted using CFDITA's ideal terminal relationships, as described in Eq. (1). The output current, I_1 obtained at terminal Z_C is given as follows.

$$I_1 = -\left[\frac{sCI_{in}-sCg_m v_{in}}{sC+g_m}\right] \quad \ldots (2)$$

If $v_{in} = 0$ in Eq. (2), then the transfer function (TF) of the filter will be given as follows.

$$\frac{I_{out}}{I_{in}} = \frac{I_1}{I_{in}} = -\frac{sC}{sC+g_m} \quad \ldots (3)$$

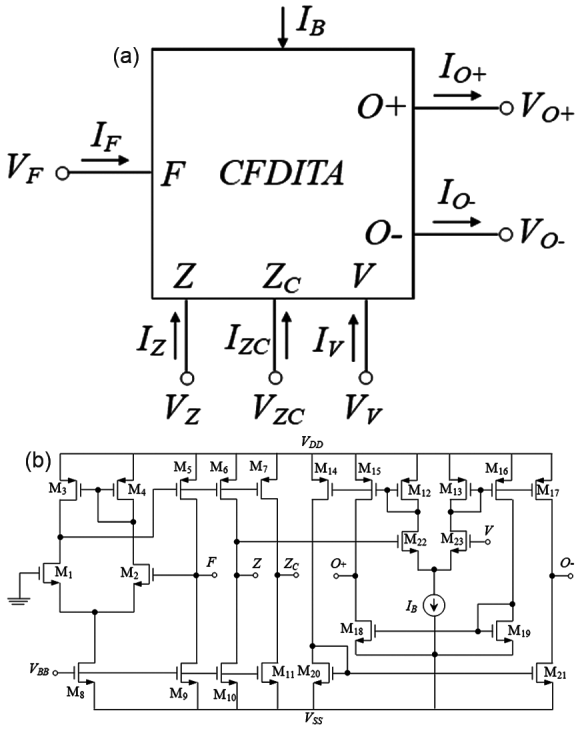

Fig. 1 — (a) Symbol of CFDITA; and (b) CMOS implementation of CFDITA

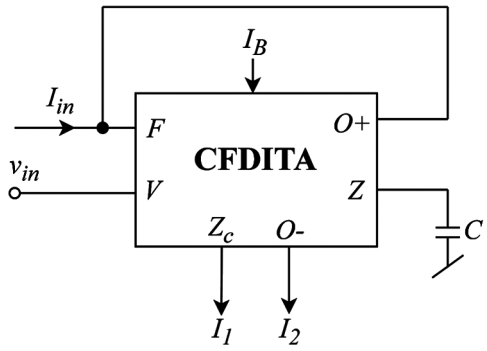

Fig. 2 — Proposed first-order mixed-mode multifunction filter

It is observed from Eq. (3), that the proposed filter realizes an inverting CM HP filter. If $I_{in} = 0$ in Eq. (2), the filter's TF will be as follows.

$$\frac{I_{out}}{v_{in}} = \frac{I_1}{v_{in}} = \frac{sCg_m}{sC+g_m} \quad \ldots (4)$$

It is observed from Eq. (4), that the proposed filter realizes a non-inverting TAM HP filter. The output current, I_2 obtained from terminal *O*- of the suggested filter is given as follows.

$$I_2 = \frac{g_m I_{in} + sCg_m v_{in}}{sC+g_m} \quad \ldots (5)$$

If $v_{in} = 0$ in Eq. (5), then the TF of the filter will be as given below.

$$\frac{I_{out}}{I_{in}} = \frac{I_2}{I_{in}} = \frac{g_m}{sC+g_m} \quad \ldots (6)$$

It is observed from Eq. (6), that a non-inverting CM LP filter is realized with the suggested circuit. Under the condition, $I_{in} = 0$ in Eq. (5), the realized TF of the filter will be a non-inverting TAM HP filter and its expression will be the same as expressed in Eq. (4).

If the output signal currents, I_1 and I_2 are connected together, the expression of the combined current signal will be given as follows.

$$I_1 + I_2 = \frac{-(sC-g_m)I_{in} + 2sCg_m v_{in}}{sC+g_m} \quad \ldots (7)$$

An inverting CM AP filter TF can be obtained as follows under the condition that $v_{in} = 0$ in Eq. (7).

$$\frac{I_{out}}{I_{in}} = \frac{I_1+I_2}{I_{in}} = -\left[\frac{sC-g_m}{sC+g_m}\right] \quad \ldots (8)$$

The realized AP filter's phase response is calculated as follows.

$$\varphi(\omega) = 180° - 2\,tan^{-1}\left(\frac{\omega C}{g_m}\right) \quad \ldots (9)$$

Based on Eq. (9), the AP filter is capable of phase shifting from 0° (at ω=0) to -180° (at ω=∞).

Under the condition, $I_{in} = 0$ in Eq. (7), a non-inverting TAM HP filter TF with a gain of 2 can be realized as given below.

$$\frac{I_{out}}{v_{in}} = \frac{I_1+I_2}{I_{in}} = \frac{2sCg_m}{sC+g_m} \quad \ldots (10)$$

The pole frequency, f_0 of all the realized TF is expressed as given below.

$$f_0 = \frac{g_m}{2\pi C} \quad \ldots (11)$$

The transconductance of CFDITA may be readily adjusted by bias current I_B to electronically tune the f_0. The cut-off frequency's sensitivities with respect to g_m and C are found to be unity in magnitude, as given below.

$$S_{g_m}^{f_o} = -S_C^{f_o} = 1 \quad \ldots (12)$$

2.2 Non-ideal and Parasitic Analysis

Considering non-ideal aspects of CFDITA, the port relationships of CFDITA are modified and described in the following matrix.

$$\begin{bmatrix} I_V \\ I_Z \\ I_{Zc} \\ I_{O+} \\ I_{O-} \end{bmatrix} = \begin{bmatrix} 0 & 0 & 0 \\ 0 & 0 & \alpha_1 \\ 0 & 0 & \alpha_2 \\ -\gamma_1 g_m & \gamma_1 g_m & 0 \\ \gamma_2 g_m & -\gamma_2 g_m & 0 \end{bmatrix} \begin{bmatrix} V_V \\ V_Z \\ I_F \end{bmatrix} \quad \ldots (13)$$

where α_1, α_2 are non-ideal current transfer gain from terminal F to terminal Z and Z_C respectively; γ_1 and γ_2 are non-ideal inaccuracies in transconductance from terminal Z to $O+$ and $O-$ respectively. The CFDITA also exhibits several parasitic elements, including a series resistance R_F at the F terminal and a parallel combination of a resistance R_i and a capacitance C_i at the i^{th} terminal, where $i = Z$, Z_C, V, $O+$, $O-$. Considering the parasitic effects alongside the nonidealities of (13), the constructed FO-MMMF filter circuit is reassessed. The expression of the current signal, I_1 is now revised as given below.

$$I_1 = -\left[\frac{\alpha_2 sC' I_{in} - \alpha_2\gamma_1 sC' g_m v_{in}}{sC' + \alpha_1\gamma_1 g_m}\right] \quad \ldots (14)$$

where $C' = C + C_Z$. The capacitance C_Z is the parasitic capacitance of Z terminal. The CM TF given in Eq. (3) is now modified as follows.

$$\frac{I_{out}}{I_{in}} = \frac{I_1}{I_{in}} = -\left[\frac{\alpha_2 sC'}{sC' + \alpha_1\gamma_1 g_m}\right] \quad \ldots (15)$$

The TAM TF given in Eq. (4) is now changed as given below.

$$\frac{I_{out}}{v_{in}} = \frac{I_1}{v_{in}} = \frac{\alpha_2\gamma_1 sC' g_m}{sC' + \alpha_1\gamma_1 g_m} \quad \ldots (16)$$

The output current, I_2 can now be expressed as below.

$$I_2 = \frac{\alpha_1\gamma_2 g_m I_{in} + \gamma_2 sC' g_m v_{in}}{sC' + \alpha_1\gamma_1 g_m} \quad \ldots (17)$$

The CM LP filter TF given in Eq. (6) is now modified as follows.

$$\frac{I_{out}}{I_{in}} = \frac{I_2}{I_{in}} = \frac{\alpha_1\gamma_2 g_m}{sC' + \alpha_1\gamma_1 g_m} \quad \ldots (18)$$

The TAM HP filter TF obtained from Eq. (17) is expressed below.

$$\frac{I_{out}}{v_{in}} = \frac{I_2}{v_{in}} = \frac{\gamma_2 sC' g_m}{sC' + \alpha_1\gamma_1 g_m} \quad \ldots (19)$$

The AP TF given in Eq. (8) is now modified as follows.

$$\frac{I_{out}}{I_{in}} = \frac{I_1 + I_2}{I_{in}} = -\left[\frac{\alpha_2 sC' - \alpha_1\gamma_2 g_m}{sC' + \alpha_1\gamma_1 g_m}\right] \quad \ldots (20)$$

The TAM HP filter TF, obtained by combining current signals I_1 and I_2, expressed in (10), is now revised as follows.

$$\frac{I_{out}}{v_{in}} = \frac{I_1 + I_2}{I_{in}} = \frac{\alpha_2\gamma_1 sC' g_m + \gamma_2 sC' g_m}{sC' + \alpha_1\gamma_1 g_m} \quad \ldots (21)$$

As a result, the suggested filter's pole frequency is updated as follows.

$$f_0 = \frac{\alpha_1\gamma_1 g_m}{2\pi C'} \quad \ldots (22)$$

The pole frequency is affected by the non-ideal gains and parasitic of CFDITA. However, the effect of parasitic can be minimized by selecting external capacitor value such as $C >> C_Z$.

3 Simulation Results

Post-layout simulations utilizing the Cadence Virtuoso tool with a 180 nm GPDK (Generic Process Design Kit) technology are included to verify the proposed circuit. Post-layout simulations take into account the parasitic of the active block used, making them closely aligned with the experimental results[38-39]. The aspect ratios of MOS are given as follows: M_1–M_2, M_5-M_6, M_7: W/L = 0.36/0.18, M_3–M_4: W/L = 1.44/0.18, M_8–M_{11}: W/L =16.2/0.18, M_{12}–M_{17}, M_{22}–M_{23}: W/L = 9/0.18, M_{18}–M_{21}: W/L = 1/0.18. The layout of CFDITA, which occupy an area of 28.4 µm × 26.5 µm, is illustrated in Fig. 3. The supply voltages of ±1.25 V and biasing current I_B = 90 µA are used to verify the proposed CM filter. The capacitor value of 15 pF is selected for the intended pole frequency of 10.6 MHz. Figures 4 (a) and (b) depict the simulated gain responses of the CM LP filter and HP filter, respectively. The transient response of the LP filter at 100 kHz and the HP filter at 100 MHz are presented in Fig. 5 (a) and (b), respectively. Fig. 5 confirms that the realized LP filter is an inver ting type and the HP filter is a non-inverting type. The suggested CM filter is now configured as an AP filter, and its gain and phase plots are depicted in Fig. 6. It is also discovered

that the simulated pole frequency is 10.3 MHz, which is nearly identical to the intended value. Furthermore, by simulating the phase response at three distinct bias current values, Fig. 7 illustrates the essential feature of the suggested AP filter, which is electronic tuning

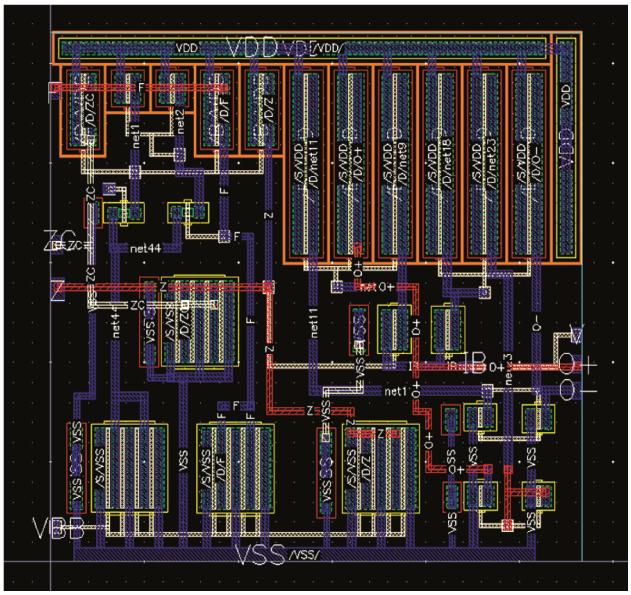

Fig. 3 — Layout of the CFDITA

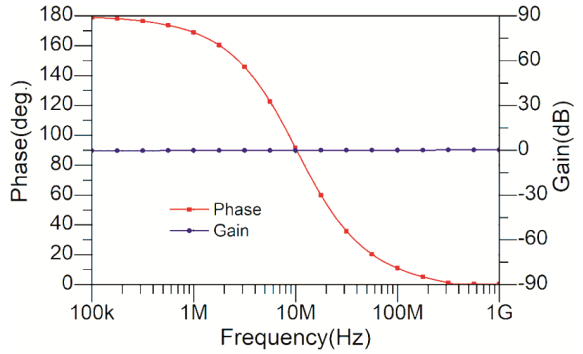

Fig. 6 — Gain and phase plot of CM AP filter

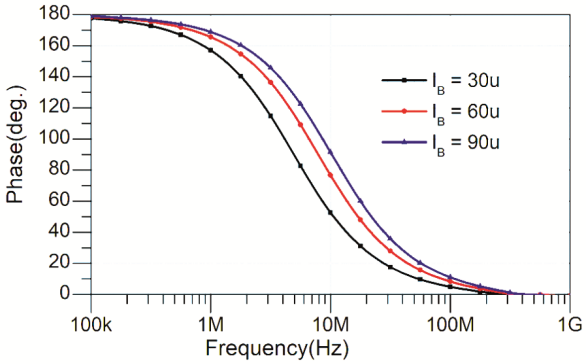

Fig. 7 — Phase variation with I_B for CM AP filter

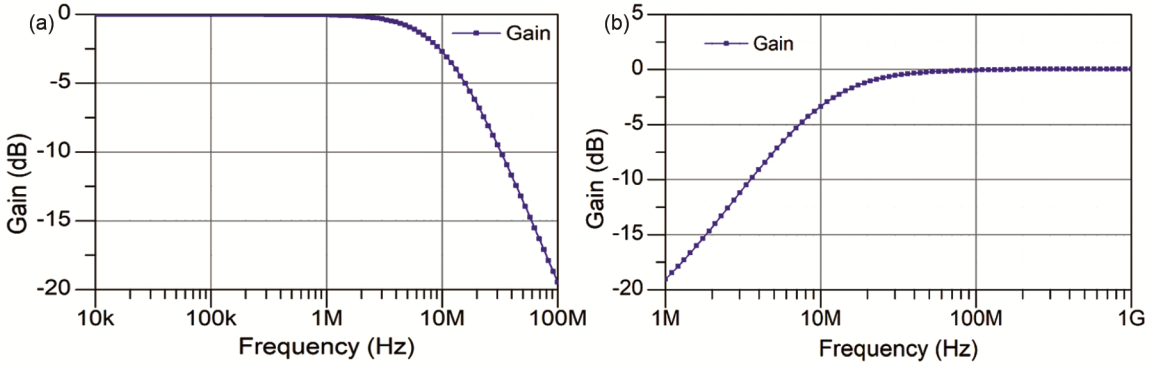

Fig. 4 — Gain responses for CM LP and HP filters

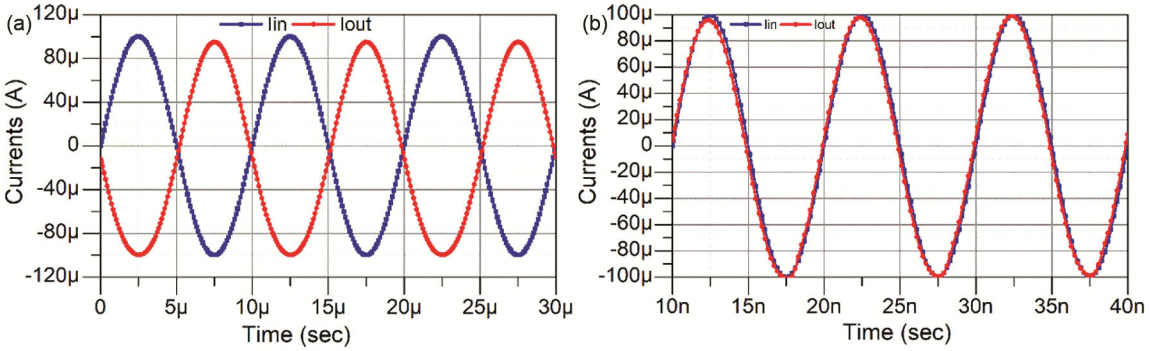

Fig. 5 — Transient responses of CM (a) LP at 100 kHz frequency; and (b) HP at 100 MHz frequency

of the pole frequency by bias current, I_B. At bias current I_B = 30 µA, 60 µA and 90 µA, the pole frequency is determined to be 4.9 MHz, 7.9 MHz and 10.3 MHz, respectively. Figure 8 shows the time domain responses of the AP filter for currents, I_{in} and I_{out} at pole frequency. At pole frequency, a quadrature relationship between currents, I_{in} and I_{out} is seen. The performance of the implemented circuit against process variation and MOS transistors' mismatch is examined using Monte Carlo simulation (MCS) analysis. A total of 100 runs of MCS with random sampling are carried out. Figure 9 illustrates the MCS outcomes shown as a histogram of oscillation frequency, while Fig. 10 presents the MCS results as a histogram of the peak output current values, considering process variation and mismatches in MOS transistors. The average frequency in Fig. 9 is 10.42 MHz, whereas mean value of peak current in Fig. 10 is 99.92 µA. Figures. 9 and 10 confirm that the suggested filter has good performance against process variation and MOS transistors' mismatch. We also investigate the temperature effects on the proposed filter. Figures 11 and 12, respectively illustrate the phase responses and transient responses at various temperatures ranging from 0 to 75 °C with a step size of 25 °C. Figure 11 and 12 confirm that the suggested circuit is less affected by the temperature variation. After the successful simulation of CM filters, the suggested filter is configured as a TAM filter. The gain plot of the TAM HP filter is shown in Fig. 13. Its transient response at 100 MHz is depicted in Fig. 14.

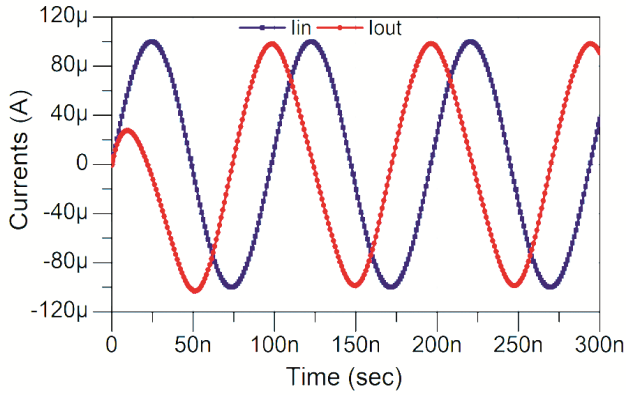

Fig. 8 — Transient plots of I_{in} and I_{out} for AP filter

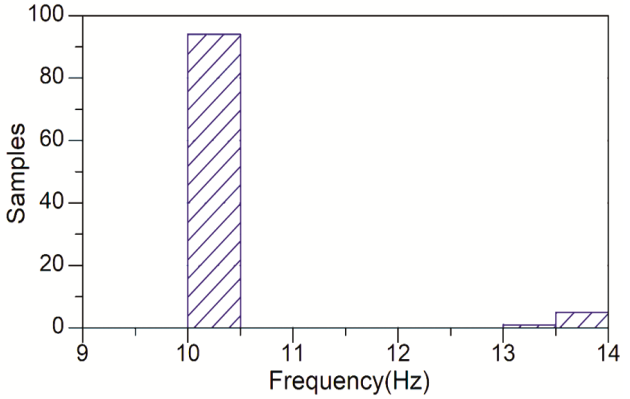

Fig. 9 — MCS results depicting a histogram of oscillation frequency

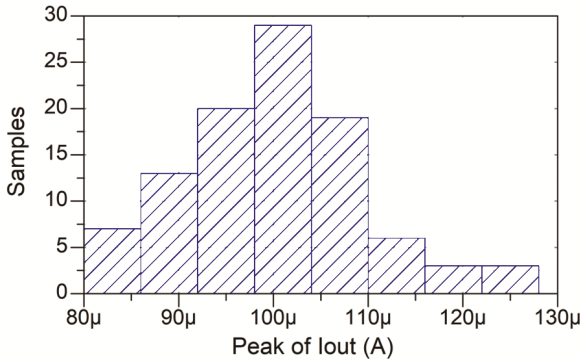

Fig. 10 — MCS results depicting a histogram of the peak of output current

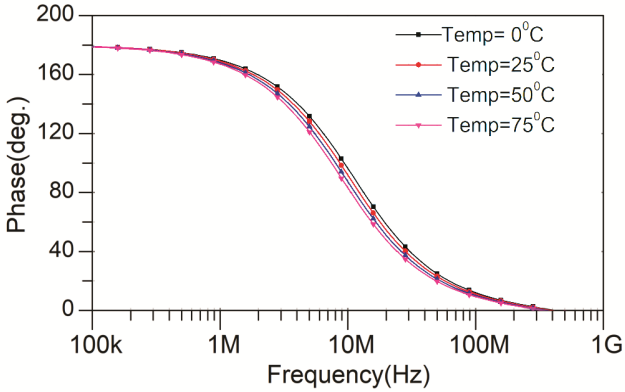

Fig. 11 — Phase variation of AP filter with temperature

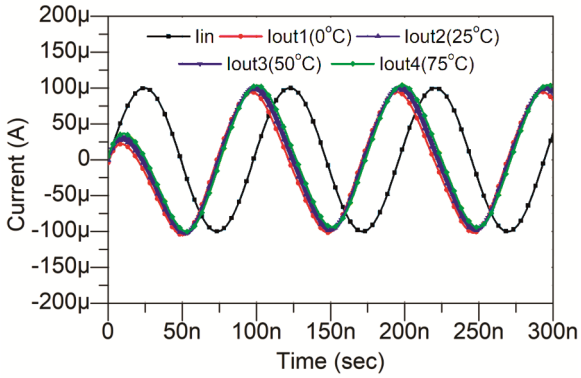

Fig. 12 — Transient plots of I_{in} and I_{out} at different temperatures

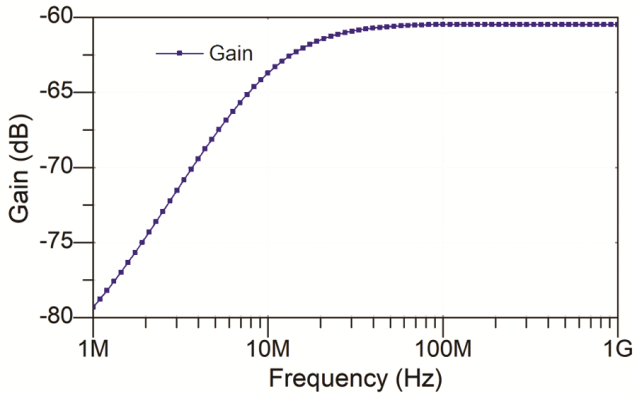

Fig. 13 — Gain response for TAM HP filter

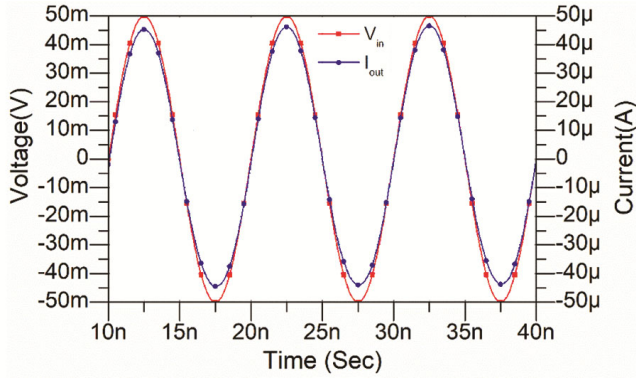

Fig. 14 — Transient response for TAM HP filter

4 Application of the Proposed Filter as Oscillator

The suggested CM filter can be effectively configured to function as a sinusoidal quadrature oscillator, as depicted in Fig. 15 (a) and (b). The suggested oscillator circuits employ two CFDITA blocks along with two capacitors, C_1 and C_2. The implemented oscillator circuits have the benefits of use of grounded capacitors only (2nd structure), resistorless realizations, and quadrature output currents, one of which is available explicitly via high impedance terminals. The $CFDITA_2$ realizes an inverting integrator, and it provides a positive feedback signal to $CFDITA_1$. Both oscillator circuits' conventional circuit analyses provide the same characteristic equation, which is shown below.

$$s^2C_1C_2 + s(g_{m1}C_2 - g_{m2}C_1) + g_{m1}g_{m2} = 0 \quad \ldots (23)$$

where g_{m1} and g_{m2} are the transconductances of $CFDITA_1$ and $CFDITA_2$ respectively. The characteristic equation of (23) can be simplified as follows for equal capacitor values, $C_1 = C_2 = C$.

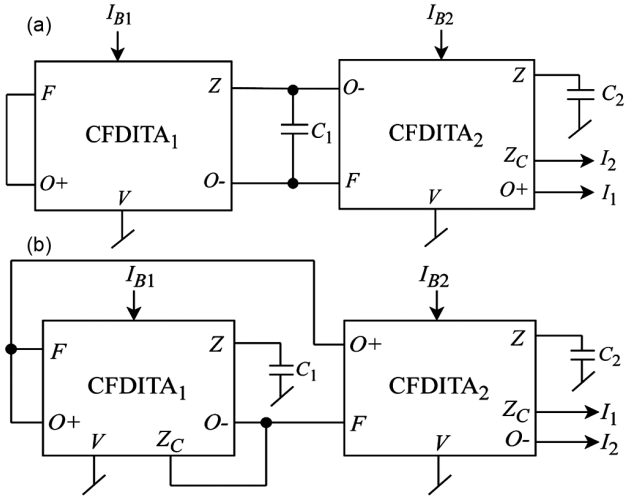

Fig. 15 — CM sinusoidal oscillator

$$s^2C^2 + sC(g_{m1} - g_{m2}) + g_{m1}g_{m2} = 0 \quad \ldots (24)$$

From Eq. (24), the condition of oscillation (CO) and the Frequency of oscillation (FO) are obtained as given below.

$$\text{CO: } g_{m1} \leq g_{m2} \quad \ldots (25a)$$

$$\text{FO: } f_o = \frac{\sqrt{g_{m1}g_{m2}}}{2\pi C} \quad \ldots (25b)$$

While taking $g_{m1} = g_{m2} = g_m$ in Eq. (23), the modified equation is as follows.

$$s^2C_1C_2 + sg_m(C_2 - C_1) + {g_m}^2 = 0 \quad \ldots (26)$$

Equation Eq. (26) gives the following CO and FO.

$$\text{CO: } C_2 \leq C_1 \quad \ldots (27a)$$

$$\text{FO: } f_0 = \frac{g_m}{2\pi\sqrt{C_1C_2}} \quad \ldots (27b)$$

The implemented sinusoidal oscillator circuits are simulated with capacitor values of $C_1 = C_2 = 150$ pF, and transconductances are chosen as $g_{m1} = 0.65$ mS and $g_{m2} = 1$ mS. The simulated output waveforms and their frequency spectrums are illustrated in Fig. 16. The simulated steady-state oscillation frequency is measured as $f_0 = 0.84$ MHz. Figure 17 depicts the transient waveforms and frequency spectrums at $f_0 = 8.4$ MHz when capacitor values are changed to $C_1 = C_2 = 15$ pF. The simulated output waveforms for currents I_1 and I_2 have total harmonic distortions of 0.81 % and 0.93 %, respectively.

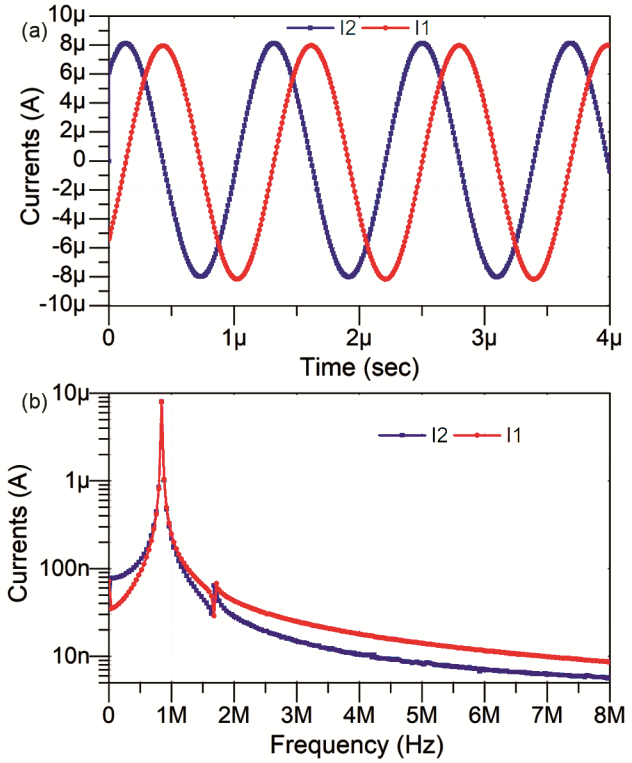

Fig. 16 — Simulation results for currents, I_1 and I_2 (a) Transient plots; and (b) Frequency spectrums at 0.84 MHz

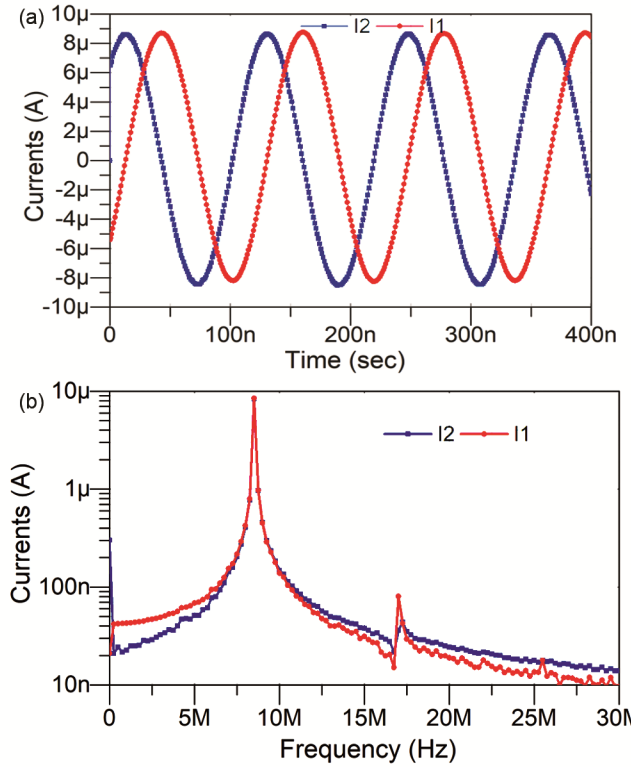

Fig. 17 — Simulation results for currents, I_1 and I_2 (a) Transient plots; and (b) Frequency spectrums at 8.4 MHz

5 Conclusion

A FO-MMMF has been presented, which consists of a single CFDITA and one grounded capacitor. This filter design is capable of providing CM LP, HP, and AP filter functions, along with a TAM HP filter function. The study has addressed the ideal and non-ideal analyses of the proposed circuit. The filter design demonstrates excellent accuracy and effective electronic tunability through modulation of bias current. Monte Carlo simulations and thermal analysis have confirmed the circuit's resilience against process and thermal fluctuations. Additional notable features of the proposed FO-MMMF filter include a compact circuit design, reduced sensitivity to device parasitic, the capability to drive loads efficiently in both CM and TAM, ease of cascading, and operation at low voltage (± 1.25 V), higher operating frequency (10.3 MHz) and low power (1.5 mW), An application of the designed filter is a sinusoidal oscillator, which shows stable oscillations with a total harmonic distortion within 1% only. The performance of the suggested filter and oscillator circuits has been validated through post-layout simulations conducted using Cadence Virtuoso. The results indicate outstanding performance, making the proposed design appropriate for various analog signal processing applications.

References

1 Smith K C & Sedra A S, *Proceedings of the IEEE*, 56 (1968) 1368.
2 Sedra A S & Smith K C, 17 (1970) 132.
3 Chaturvedi B, Kumar A & Mohan J, *AEU-Int Electr Comm*, 99 (2019) 110.
4 Kumngern M, Jongchanachavawat W, Phatsornsiri P, Wongprommoon N, Khateb F & Kulej T, *Electron*,12 (2023) 2828.
5 Kumar A, Kumar S, Elkamchouchi D H & Urooj S, *Electron,* 11 (2022) 2072.
6 Maheshwari S, *IET Circuits, Devices & Syst*, 12 (2018) 478.
7 Agrawal D & Maheshwari S, *J Circuits, Syst Comp*, 28 (2019) 1950219.
8 Kumar A & Chaturvedi B, *Iran J Electric Electr Eng*, 2 (2018) 162.
9 Singh B & Maheshwari S, *Int Conference on Smart Electronics and Communication (ICOSEC)*, (2020) 1301-1305.
10 Bansal K, Mohan J & Chaturvedi B, In *Proceedings of the 2024 Sixteenth International Conference on Contemporary Computing*, (2024) 762-767.
11 Kumar A & Chaturvedi B, *International Conference on Signal Processing and Communication (ICSC)*, (2016) 229-232.
12 Chaturvedi B, Mohan J, Jitendra & Kumar A, *Radio Sci*, 55 (2020) 1.

13 Chaturvedi B, Mohan J, Kumar A & Pal K, *J Circuits, Syst Comp*, 29 (2020) 2050149.

14 Herencsar N, Koton J, Minaei S, Yuce E & Vrba K, *International Conference on Electrical and Electronics Engineering (ELECO),* (2011) 141-154.

15 Chaturvedi B, Mohan J & Gupta SN, *e-Prime-Advances in Electrical Engineering, Electronics and Energy*, 4 (2023) 100165.

16 Uttaphut P, *Przegląd elektrotechniczny*, 95 (2019) 101.

17 Bansal K, Mohan J & Chaturvedi B, *Recent Patents Eng*, 20 (5) (2024) 15.

18 Das R, Parween G, Mumtaz B & Reyaz A, *Int J Eng Develop Res* 7, 1 (2019) 220.

19 Kumar A, Kushwaha A K & Paul S K, *Adv Power Syst Energy Managem (ETAEERE)*, 436 (2018) 709.

20 Jitender, Mohan J & Chaturvedi B, *6th International Conference on Signal Processing and Communication (ICSC)*, (2020) 235-239.

21 Jitender, Mohan J & Chaturvedi B, *Walailak J Sci Technol (WJST)*, 18 (2021) 21451.

22 Konal M & Kacar F, *Analog Integr Circuits Signal Process*, 108 (2021) 173.

23 Senani R, Bhaskar D R & Kumar P, *AEU-Int J Electr Commun*,137 (2021) 153742.

24 Yuce E, Verma R, Pandey N & Minaei S, *AEU-Int J Electr Commun*, 103 (2019) 57.

25 Mohan J, Chaturvedi B & Kumar A, *J Circuits, Syst Comp*, 30 (2021) 2150268.

26 Lawate S V, Hajare P R & Kimmatkar M S, *J Algebraic Statistics*,13 (3) (2022) 5552.

27 Singh G, *Circuits Syst*, 11 (2020) 39.

28 Chaturvedi B & Kumar A, *Circuits, Syst Signal Process*, 38 (2019) 2.

29 Perumal S, Faseehuddin M, Kukker A, Shireen S & Tangsrirat W, *Inform MIDEM*, 53 (2023) 177.

30 Yuce E, Safari L, Minaei S, Ferri G & Stornelli V, *IET Circuits, Devices Syst*, 14 (2020) 901.

31 Roongmuanpha N, Likhitkitwoerakul N, Fukuhara M & Tangsrirat W, *Sensors*, 23 (2023) 2759.

32 Faseehuddin M, Sampe J, Shireen S & Md Ali S H, *J Circuits, Syst Comp*, 29 (2020) 2050078.

33 Kumar A & Chaturvedi B, In *2016 International Conference on Signal Processing and Communication (ICSC)*, IEEE , (2016) 374-379.

34 Chaturvedi B & Kumar A, *IET Circuits, Devices & Syst*, 12 (2018) 817.

35 Kumar A, Chaturvedi B & Jagga S, *Circuits, Syst, Signal Proc*, 42 (2023) 1911.

36 Kumar A, Chaturvedi B & Jagga S, *J Integr Circuits Syst*, 19 (2024) 1.

37 Kumar A, *IETE J Res*, 70 (2024) 708.

38 Shankar C & Singh SV, *Indian J of Pure Appl Phys (IJPAP)*, 57 (2019) 52.

39 Kumar A, *J Circuits, Syst Comp*, 30 (2021) 2150107.